Egyptian Geophysical Society
EGS Journal, Vol. 16, No. 1, 71-81 (2018)

ANALYSIS AND INTERPRETATION OF AIRBORNE GAMMA RAY SPECTROMETRIC DATA FOR EAST WADILIGAN AREA, CENTRAL EASTERN DESERT, EGYPT

A.A. ISMAIL[(1)], S.E.A. MOUSA[(2)], A.M. MOSTAFA[(1)], S.H. ABDAL NABI[(2)] and M.A. SAYED[(3)]

(1) Airborne Geophysics Dept., Exploration Division, Nuclear Material Authority, P.O. Box 530, Maadi, Cairo, Egypt.
(2) Geophysics Department, Faculty of Science, Ain Shams University, Cairo, Egypt.
(3) Geophysics Department, Exploration Division, North Bahariya petroleum Company, Zahraa El Maadi, Cairo, Egypt.

تحليل وتفسير بيانات طيف أشعة جاما الجوية لمنطقة شرق وادي ليجان، وسط الصحراء الشرقية ، مصر

الخلاصة: تعرض هذه الدراسة تحليل وتفسير بيانات أشعة جاما الجوية لإنشاء خريطة سطحية من الوجهة الإشعاعية وتحديد المناطق الغنية بمحتوى العناصر المشعة ومقارنتها بالخريطة الجيولوجية . وقد تم تطبيق عدة خطوات متلاحقة للتحليل وتحقيق هذا الهدف و الذي تضمن بناء خريطة مركبة تجمع بين بيانات مكافىء اليورانيوم ومكافىء الثوريوم و البوتاسيوم . ثم بناء خريطة نطاقات عن طريق تقسيم المنطقة إلى نطاقات تعتمد على الفرق في اللون في الخريطة المركبة، ثم التحقق من تجانس هذه النطاقات والقدرة على جمع أو فصل كل نطاق مع مجموعة أخرى أو نطاقات من خلال تطبيق بعض العمليات الإحصائية على إجمالي البيانات الإشعاعية، بدءا من معامل الاختلاف الذى تحقق مدى تجانس كل منطقة على حدة، تليها تطبيق اختبار بارتليت وتحليل التباين (أنوفا) التي تتحقق من إمكانية تشكيل مجموعة أو مجموعات من المناطق معا ، ثم تطبيق اختبار فيشر واختبار الطالب الذي يتحقق من إمكانية تشكيل أزواج من النطاقات التي يمكن جمعها والتى تعتمد على تجانس الانحراف المعياري والمتوسط، ثم تأخذ هذه المناطق النهائية وحساب المتوسط والانحراف المعياري للبوتاسيوم ، ومكافىء اليورانيوم و مكافىء الثوريوم ثم تمثيل هذه المعاملات لثلاثة عناصر إشعاعية على خريطة واحدة ومقارنة هذه الخريطة مع الخريطة الجيولوجية.

ABSTRACT: *This study presents analysis and interpretation of airborne gamma ray data to construct surface map based on radiation point of view and determine the zones which are rich in radioelement contents and compared it with the geological map. Subsequent analysis steps were applied to achieve our target which included constructing a composite map that combines the data for eU (in red), eTh (in green), and K (in blue) then constructing a zonation map by dividing the area into zones based on difference in colour in the composite map . After that, check the homogeneity of these zones and ability to gather or separate each zone with another or groups of zones by applying some statistical operations on the total count radiometric data starting with the coefficient of variation which check the homogeneity of every zone separately. Followed by applying the Bartlett's test and analysis of variance (ANOVA) which check the possibility to form group or groups of zones together then applying the Fisher's test and the student's test which check the possibility to form couples of zones that can be gathered depending on the homogeneity of the standard deviation and the mean then taking this final zones and calculating the mean and standard deviation for the K ,eU and eTh then drawing the X+2S.D. for the three radioelements on one map and comparing this map with the geological map .*

1. INTRODUCTION

The present study area is located in the central Eastern Desert of Egypt, between latitudes 27°50′00" and 28°05′ 00" N and longitudes 32°10′00" and 32°40′00" E. The area is about 140 km East of El Miniya city (Fig.1). Aero-Service Division, Western Geophysical Company of America in 1984, carried out an airborne geophysical survey for a vast area in the Eastern Desert of Egypt including the study area in order to providing data assist in identifying and

evaluating minerals, petroleum and groundwater resources of the region. The survey was conducted along nearly parallel flight lines that were oriented in a NE-SW direction at an approximately 1.5 km space intervals, while the tie lines were flown in a NW-SE direction at 10 km intervals (Fig. 2). A system that was used in the measurements of gamma-ray is high-sensitivity 256-channel gamma-ray spectrometer system (Aero Service Report, 1984).

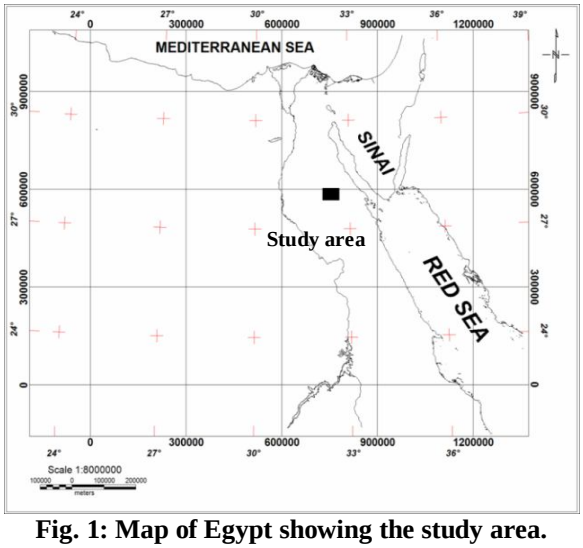

Fig. 1: Map of Egypt showing the study area.

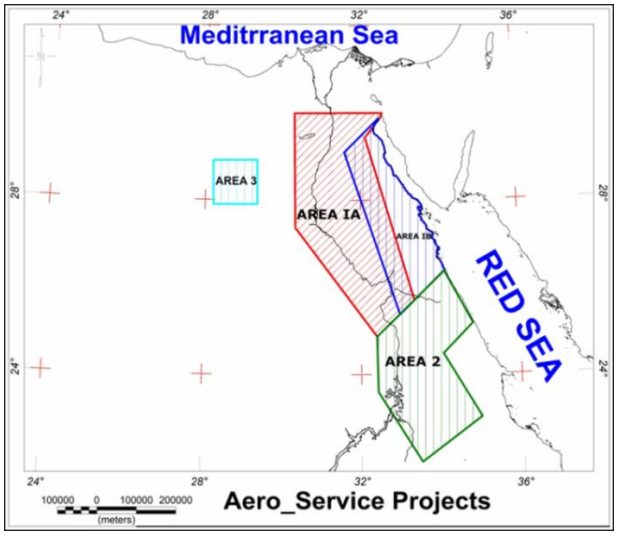

Fig. 2: Airborne Geophysical Survey Conducted by Aeroservice division, WesternGeophysical companyof America.

Raw data were subjected to some correction to be prepared to analysis and interpretation such as background correction, stripping correction, altitude correction, and conversion of count rates to ground concentrations. All corrections steps mentioned are performed by Aero-Service Company, 1984. then gridding of the radiometric data then generate the geophysical composite colour images on which each radioelement is represented by one of the three primary colours, with intensity varying according to the radioelement concentration (IAEA 1991).

The interpretation of airborne radiometric data depends on the percentages of concentrations for the three radioelements (K%, eU ppm and eTh ppm). The present study was focused on analyzing and interpreting airborne radiometric data over East WadiLigan area. The purpose of this study is to construct a surface map, which represents the radioelement concentrations for each rock type and compare it with the geological map.

2. GEOLOGICAL OUTLINES

The Central Eastern Desert displays a variation of simple and complex structural forms, so it is considered the glamorous region from the geological stand point of view. Geomorphologically, the area is dissected by several Wades at the eastern and central parts of the study area. WadiQena is located in the eastern side of the study area and has a NNW

orientation. Meanwhile WadiHawashiya and Wadi Abu Had are located in the north central corner of the study area. The lowest portion, which encountered in the south eastern part of the study area as well as GabalBerqetHamud donated by blue colour (Fig. 3), which has elevation ranging from 500 to 610 m-above sea level (asl), Also in the Middle of the southern part there are land has elevation ranging from 540 to 600 m-asl. Meanwhile, there are three high lands encountered in the area marked by pink and red colors. The first one is in the western side of the study area and reach 860 m-asl in height at G. Nihedat El Sud. The second high land is located in the central part of the study area and reaches 760 m asl. The third high land is located in the North Eastern edge of the study area and reaches 750 m asl.

The compiled geologic map (Fig. 4) clarifying the geologic rock units which varying from Pre-Cambrian basement rocks to the Quaternary deposits. The rock units are arranged according to their age from the oldest

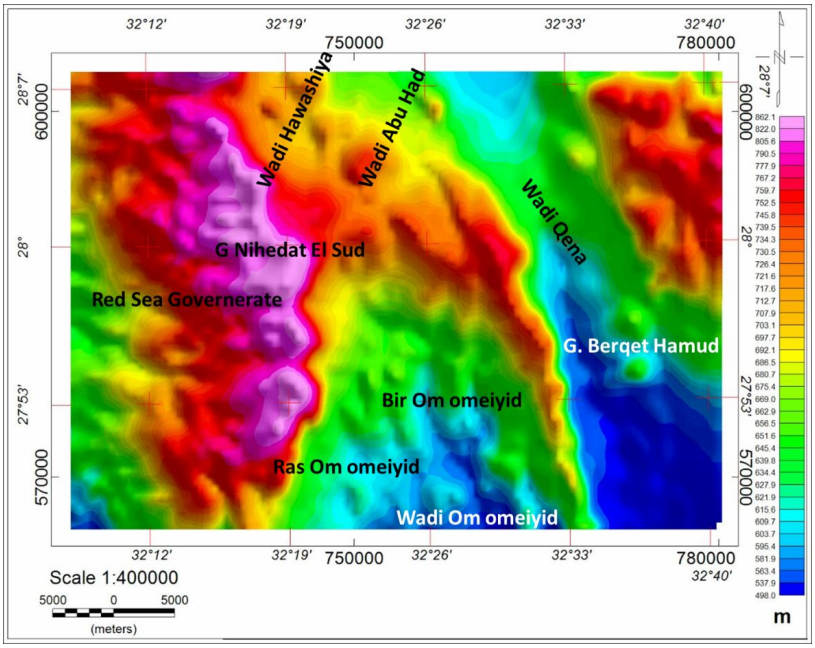

Fig. 3: Shaded color topographic map of the study area, Central Eastern Desert, Egypt.

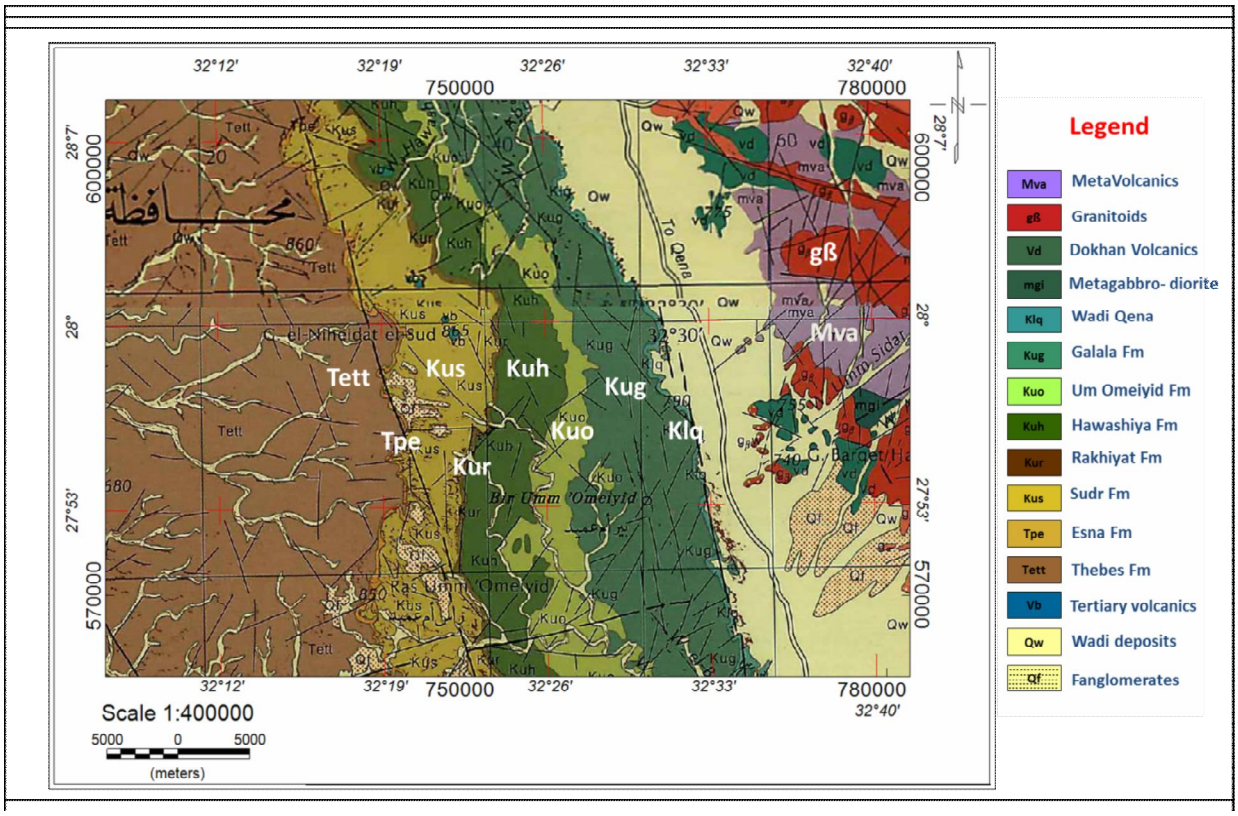

Fig. 4: Compiled geologic map of east WadiLigan area, Central Eastern Desert, Egypt, (after Conoco & EGPC, 1987).

to the newest from the east to the west. The basement complex rocks (granites, metavolcanics and Dokhanvolcanics) lie in the eastern side of the study area followed by lower Cretaceous deposits which form the most widespread rock types (about 70 % of the total area) in central and western parts of the study area and the other parts filled with Quaternary deposits.

Structurally, the central Eastern Desert of Egypt has been affected by faulting-tension- tectonism. The faults are usually normal and can be grouped into six systems: (1) 140°-150°, (2) N6°W - N2°E, (3) 12° - 20°, (4) 40°-50°, (5) 110°-120°, and (6) 70°-80°(El-Tarabili, 1964).

During the entire Paleozoic and a considerable part of the Mesozoic, the greater part of Egypt was subjected to uplift. The thrusting and /or uplifting of the north African continent against the main block of the earth's crust resulting in the formation of E-W trending swells and thrusts during Paleozoic and Jurassic times.

Sedimentary patterns from the Late Jurassic to Early Tertiary appear to have been influenced significantly by two primary tectonic forces related to Tethyan plate tectonics (Meshref 1990):

(1) The sinistral shear during the late Jurassic to Early Cretaceous (NW trending system).

(2) The dextral shear during the late Cretaceous to Paleocene time (NE trending system).

3. QUALITATIVE INTERPRETATION OF AERIAL GAMMA-RAY SPECTROMETRIC DATA

The surface concentrations of the radioelements, Potassium, Uranium and Thorium, can be quantified by measurements of intensities of gamma-ray radiation emitted by their respective radioisotopes K^{40}, Bi^{214}, and Tl^{208} (Grasty and Darnley, 1970). Such data are then used to compile maps showing the distribution of these three radioelements and their ratios. The four parameters (variables) namely: total-count of the gamma radiation (TC, in µR/h), absolute concentrations of the three radioelements, Potassium (K, in %), equivalent Uranium (eU, in ppm) and equivalent Thorium (eTh, in ppm) (Figs. 5 to 8), show relative variations of the gamma radiation. The three main radiometric elemental concentrations mainly reflect the lateral variation of surface elemental concentrations of different rock and soil types.

The radioelement composite image map (Fig. 9) combines the data for eU (in red), eTh (in green), and K (in blue) and provides on one display an overall picture of the radioelement distributions in the study area. This image offers much in terms of lithologic discrimination based on colour differences. The high level radiation combines for the three radioelements (bright areas) is encountered in the eastern, central and some scatter parts of the study area.

According to the radioelement concentrations derived from the radiometric image maps and the colour differences on the composite radioelement image maps, thirteen interpreted aerial spectral radiometric zones are clearly visible (Fig. 10), which are arranged from the east to the west of the study area. These interpreted spectral radiometric zones (ISRZ) show a fairly close spatial correlation with the mapped lithologies (Fig. 4).

Zone I : It occurs over GabalBerqetHamud and represents the middle eastern side of the study area . It is characterized by high levels of radiation encountered in the four radiometric maps (TC , K ,eTh& in eU) which is conjugated with the basement rocks (metavolcanics , metagabbro , Dokhanvolcanics and granitoids), Wadi deposits and Fanglomerate . This level could be seen as cyan colour on the composite image map (Fig. 9).

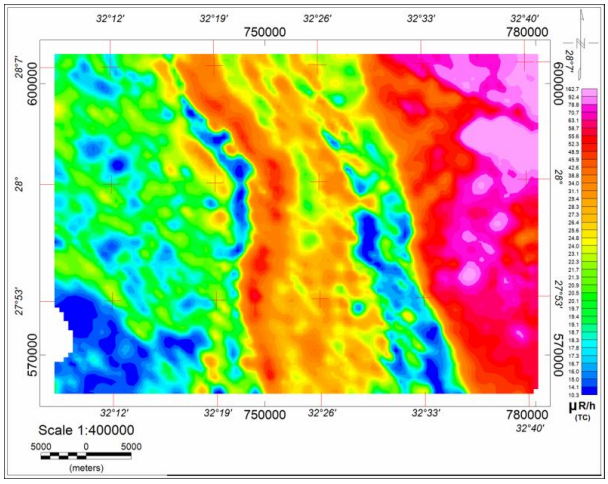

Fig. 5: False-Color Contour Map of the Total count radiometric.

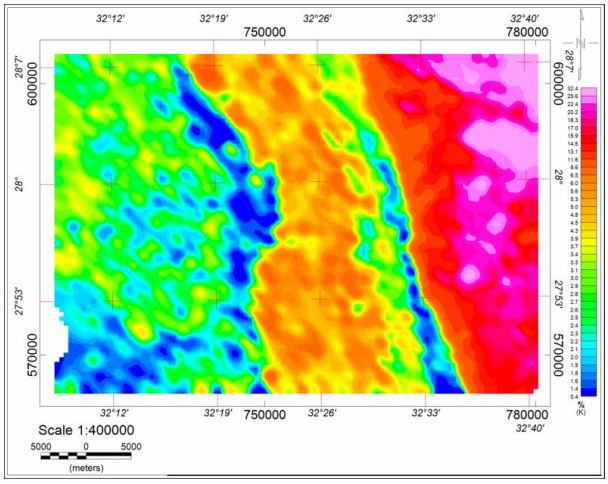

Fig. 6: False-Color Contour Map of the Potassium concentration data,EastWadiLigan Area, Central Eastern Desert, Egypt, EastWadiLigan Area, Central Eastern Desert, Egypt.

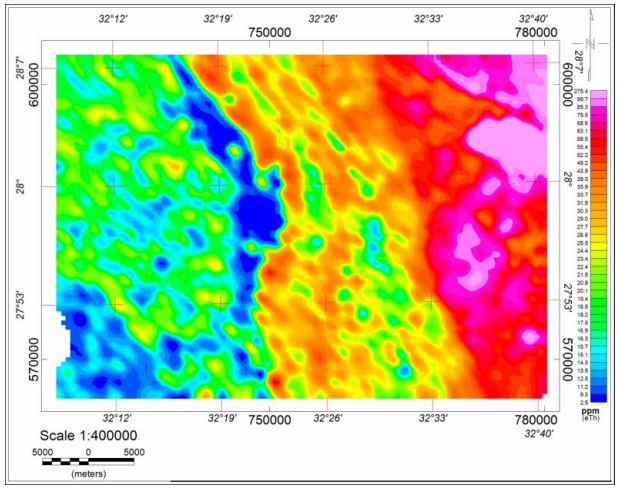

Fig. 7: False-Color Contour Map of the equivalent Uranium

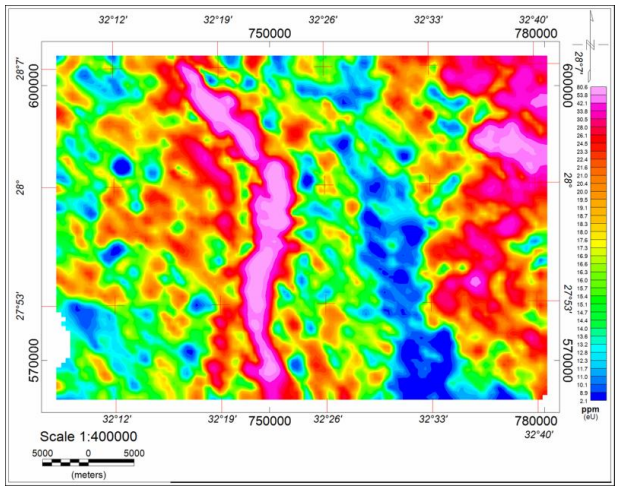

Fig. 8: False-Color Contour Map of the equivalent Thorium concentration , EastWadiLigan Area, Central Eastern Desert.concentration , EastWadiLigan Area, Central Eastern Desert.

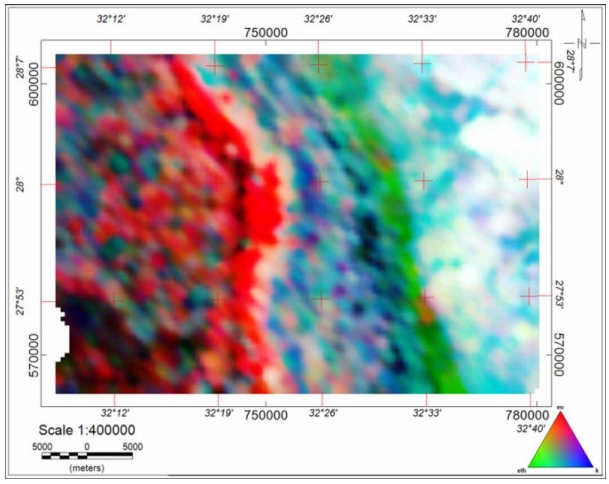

Fig. 9: False-Color Radioelement Composite Image Map, East WadiLigan area, Central Eastern Desert, Egypt.

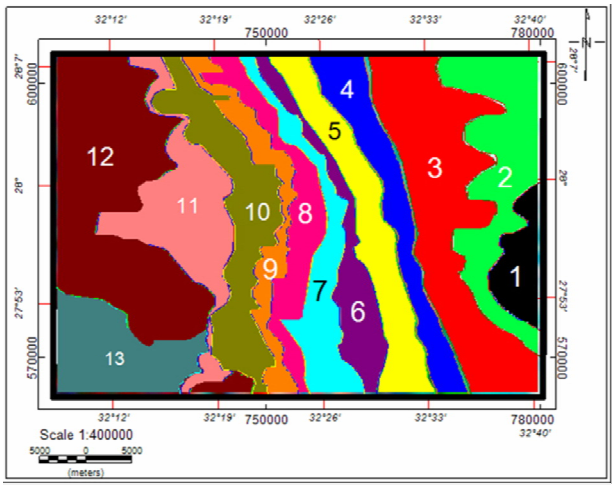

Fig. 10: Qualitative Interpreted spectral radiometric Zones Map, WadiLigan Area, Central Eastern Desert

Zone II : It occurs at the northeastern side of the study area . it is characterized by the highest level of radiation encountered in the four radiometric maps (TC , K , eTh and in eU) which is associated with the basement rocks (metavolcanics , metagabbro, Dokhan volcanics and granitoids), Wadi deposits and Fanglomerate. This level could be seen as milky colour on the composite image map (Fig. 9).

Zone III : It is characterized by relatively high level of radiation encountered in TC , K , and in eTh maps and intermediate to low values in some parts of Uranium (eU). It is mainly associated with WadiQena deposits and in some scatter parts of the basement rocks (Metavolcanics , Dokhanvolcanics and granitoids), and Fanglomerate. This level could be seen as rosy cyan colour on the composite image map (Fig. 9). This zone trends nearly in a NNW-SSE direction.

Zone IV : It is characterized by low to intermediate level of radiation encountered in the three radiometric maps TC , K , and in eU and intermediate to high values in Thorium map which is conjugated with WadiQena Formation. This level could be seen as green colour on the composite image map (Fig. 9) with a NNW-SSE direction.

Zone V : It is characterized by intermediate level of radiation encountered in the three radiometric maps in TC , K and in eTh and the low values of eU which is conjugated with Galala Formation. This level could be seen as pale blue colour on the composite image map (Fig. 9) with a NNW-SSE direction.

Zone VI : It has intermediate to high values of radiation encountered in the three radiometric mapsTC , K and in eTh and intermediate to low values over eU map. This level could be seen as rosy blue colour on the composite image map (Fig.9), which is conjugated with the Galala Formation. This zone trends nearly in a NNW-SSE direction.

Zone VII : It has intermediate to high values of radiation encountered in the three radiometric maps TC, K and in eTh and intermediate to low values over eU map. This level could be seen as rosy blue colour on the composite image map (Fig. 9), which is conjugated with the Umm umeiyid Formation. This zone trends in the NNW-SSE and N-S directions.

Zone VIII : It has intermediate to high values of radiation encountered in the three radiometric maps TC , K and in eTh and intermediate to low values over eU map. This level could be seen as rosy dark blue colour on the composite image map (Fig. 9), which is conjugated with the Hawashiya Formation. This zone trends in the NNW-SSE and N-S directions.

Zone IX : It has high values of radiation encountered in the three radiometric maps TC , K and in eTh and the high values over eU map. It is conjugated with the Rakhiyat Formation which is rich in phosphate that is characterized by high uranium content. This level could be seen as rose colour on the composite image map (Fig. 9), which trends in the NNW-SSE and N-S directions.

Zone X : It is characterized by the lowest level of radiation encountered in the Potassium and Thorium maps, intermediate to the high values over eU map and very low to very high values over TC map. This level could be seen as red colour on the composite image map (Fig. 9), which is conjugated with the sudr Formation. This zone trends in the NNW-SSE and N-S directions.

Zone XI : It has low to intermediate values of radiation encountered in the TC, K and in eTh maps and high values over eU map. This level could be seen as pale red colour on the composite image map (Fig. 9), which is conjugated with the Esna Formation and thebes formations. This zone trends in the N-S direction.

Zone XII : It occurs at the northwestern side of the study area , it is characterized by low to intermediate values of radiation encountered in the TC , K and in eTh maps and low to high values over eU map. This level could be seen as reddish pale blue colour in the composite image map (Fig. 9), which is conjugated with the Thebes Formation. This zone trends in the NW-SE and N-S directions.

Zone XIII : It represents the southwestern side of the study area , it is characterized by the lowest values of radiation encountered in the TC , K and in eTh maps and low to high values over eU map. This level could be seen as reddish dark blue colour on the composite image map (Fig.9), which is conjugated with the Thebes Formation. This zone trends in the N-S direction.

4. QUANTITATIVE INTERPRETATION OF AERIAL GAMMA-RAY SPECTROMETRIC DATA

4.1. Statistical Analysis of the Spectral Radiometric data

4.1.1. Coefficient of Variation:

In probability theory and statistics, the coefficient of variation (CV), also known as relative standard deviation (RSD), it is also known as unitized risk or the

variance coefficient, is a standardized measure of dispersion of a probability distribution or frequency distribution. It only uses positive numbers in the calculation and expressed as a percentage, Therefore, the resultant value of this formula CV = (Standard Deviation (S) / Mean (X)) will be multiplied by 100 (Everitt, Brian 1998*)* .

Based on the results of the qualitative interpretation of the airborne spectrometric data, the area under study is divided into 13 zones.

Then applying the C.V. equations on the total count data for all zones starting from zone (I) to zone (XIII) & the results are represented in table (1).

Table (1) Results of application the coefficient of variation on the TC radiometric data of East WadiLiganarea , Central Eastern Desert.

Zones	Min.	Max.	Mean	S.D.	C.V.
1	35.21	83.05	59.27	8.14	**13.73376076**
2	45.47	165.81	87.38	25.28	**28.93110552**
3	17.98	83.98	50.38	9.52	**18.89638746**
4	11.56	32.54	19.98	3.66	**18.31831832**
5	10.69	36	20.74	4.77	**22.99903568**
6	14.66	35.28	26.48	3.48	**13.14199396**
7	21.56	40.18	28.16	2.67	**9.481534091**
8	18.16	38.48	25.56	3.36	**13.14553991**
9	23.78	61.19	38.02	7.12	**18.7269858**
10	11.77	56.15	26.62	10.28	**38.61758077**
11	14.55	35.66	21.13	3.01	**14.24514908**
12	11.22	27.81	19.2	1.89	**9.84375**
13	10.03	23.78	15.4	2.11	**13.7012987**

The results of C.V. are less than 100 in all zones that were founded in the area and depend on the radioelement contents so every zone separately represents a homogeneous medium.

4.1.2. Application of Inference Tests

a. Bartlett's test:

Variance of all units were arranged into increasing order (Table 2). The unit or units having the most distant variance or variances were excluded, and the test for homogeneity of variances was applied again. This iterative process of removal of the most deviant variance is stopped when the test is accepted.

$B=M/C$

$M = 2.3026\ (N.\log sa^2 - D)$

$D = \sum_{i=1}^{i=k} (ni.\log si^2)$

$N = \sum_{i=1}^{i=k} ni$

$$S_a^2 = \frac{\sum_{i=1}^{i=k} (n_i * S_i^2)}{N}$$

$$C = 1 + \frac{1}{3(K-1)} \left(\sum_{i=1}^{i=k} \frac{1}{ni} - \frac{1}{N}\right)$$

where

ni= number of data for each sample

N = number of data for all sample

K = number of samples

Sa = variance within each of the samples

Si= Sample variance

As a result of this iterative procedure, 11 groups were tested for total-count radiometric data (Table 3).

The assumption of homogeneity of variances was rejected for the groups when calculated test values exceeded the critical values (Geigy, 1962).

As a result, all 11 groups were rejected. Differences between variances of these groups were significant statistically and, therefore, these units were considered to possess heterogeneous variances in terms of radioactivity at the 95 % level of confidence.

Table 2: Arrangement of the standard deviation on the TC radiometric data of East WadiLigan area , Central Eastern Desert, Egypt.

Zones	S.D.
12	1.89
13	2.11
7	2.67
11	3.01
8	3.36
6	3.48
4	3.66
5	4.77
9	7.12
1	8.14
3	9.52
10	10.28
2	25.28

Table 3: Results of application the bartlett's test on the TC radiometric data of East WadiLigan area , Central Eastern Desert, Egypt.

Zones	B calculated	B critical	Results
1-13	**316065**	21.03	**Rejected**
2-13	**156025.45**	19.68	**Rejected**
3-13	**132367.6**	18.31	**Rejected**
4-13	**66160.295**	16.92	**Rejected**
5-13	**50133.285**	15.51	**Rejected**
6-13	**28659.462**	14.07	**Rejected**
7-13	**16626.041**	12.59	**Rejected**
8-13	**13163.961**	11.07	**Rejected**
9-13	**10680.553**	9.49	**Rejected**
10-13	**7383.7955**	7.81	**Rejected**
11-13	**2684.514**	5.99	**Rejected**

b. Analysis of Variances test (ANOVA):

Following the previous test, it was necessary to test the homogeneity of mean background radioactivities of the units constituting more than two groups proved to possess comparable variances. This was performed by applying the Analysis of Variance test (ANOVA), (Dixon and Massey, 1957).

The analysis comprises the computation of both the variance between the samples *Sm* , and the variance within each of the samples *Sp*. where

$$S_m^2 = \frac{\sum_{i=1}^{i=k} n_i (x_i - x_m)^2}{k - 1}$$

where *k* = number of samples

ni= the number of data in each sample

Xm= is the mean of the means

Xi = is the mean for each sample

$$S_p^2 = \frac{\sum_{i=1}^{i=k} (n_i - 1) * S_i^2}{N - K}$$

The *R* ratio is used to test the significant difference where,

$$R = R = S_m^2 / S_p^2$$

Due to the results of the bartlett's test which proved the heterogeneity of the variances so the Anova test can't be applied.

c. Fisher's (F-) test:

The relations between each pair of rock units possessing comparable variances were tested by using F-test.

The procedure is to take two neighboring samples from the population zone that arranged ascending based on the standard deviation (Table 2) and compute the ratio of the sample variances.

$$F = S_1^2 / S_2^2$$

In which the larger of the two sample variances is always to be made the numerator.

If the test (F-ratio) value is smaller than the critical one for (k-1) and (n1+n2-2) degrees of freedom, then the assumption of equal variances is accepted at the 95% level of confidence. Otherwise, if the value of F-ratio exceeds the critical one, the hypothesis of homogeneous variances is rejected (Geigy, 1962).

As a result, 11 couples were accepted for total-count radiometric (Table 4). The remaining couple (Table 4) was considered to possess heterogeneous variances in terms of radioactivity at the 95% level of confidences.

d. Student's test:

It is used to test the hypothesis of the homogeneity of the means of two normally distributed and independent sample means (*X1* and *X2*) when their variances (*S1* and *S2*) were proved to be homogeneous, with a statistic test "t" which is given by:

$$t = \frac{X_1 - X_2}{S_p \sqrt{(1/n1) + (1/n_2)}}$$

where

$$S_p^2 = \frac{(n_1 - 1) * S_1^2 + (n_2 - 1) * S_2^2}{(n_1 + n_2 - 2)}$$

when the computed test value was higher than the critical one for (n1+ n2 -2) degree of freedom, the assumption of equal means was rejected at 95% level of significance and was accepted when the former value is below the latter one (Geigy, 1962). The hypothesis of equal mean of the 11 couples accepted from applying F-test are rejected according to the results of t-test (Table 4).

Table 4: Results of application the Fisher's test & T-test on the TC radiometric data of East WadiLiganarea, central eastern desert, Egypt.

Groups	F calculated	F critical	Results	T calculated	T critical	Results
12&13	**1.246354**	3.85	**Accepted**	**100.6243**	1.96	**Rejected**
13&7	**1.601244**	3.85	**Accepted**	**179.4446**	1.96	**Rejected**
7&11	**1.270897**	3.85	**Accepted**	**76.89938**	1.96	**Rejected**
11&8	**1.246079**	3.85	**Accepted**	**40.09204**	1.96	**Rejected**
8&6	**1.072704**	3.85	**Accepted**	**5.968883**	1.96	**Rejected**
6&4	**1.106124**	3.85	**Accepted**	**39.36717**	1.96	**Rejected**
4&5	**1.698535**	3.85	**Accepted**	**3.625412**	1.96	**Rejected**
5&9	**2.228041**	3.85	**Accepted**	**41.33641**	1.96	**Rejected**
9&1	**1.30704**	3.85	**Accepted**	**23.28244**	1.96	**Rejected**
1&3	**1.367808**	3.85	**Accepted**	**7.574443**	1.96	**Rejected**
3&10	**1.166037**	3.85	**Accepted**	**27.70369**	1.96	**Rejected**
10&2	**6.047389**	3.85	**Rejected**			

Table (5): Statistical analysis of Potassium distribution in (%) for each zone in East WadiLigan area

Zones	Min.	Max.	Mean	S.D.	X+3 S.D.	X+2 S.D.	X+S.D.
1	**11.45**	**25.5**	**17.69**	**2.26**	**24.47366**	**22.21453**	**19.9554**
2	**11.9**	**32.55**	**22.9**	**4.05**	**35.07927**	**31.02498**	**26.97068**
3	**2.85**	**24.37**	**13.87**	**3.38**	**24.01212**	**20.63283**	**17.25354**
4	0.43	7.23	2.63	0.97	**5.540414**	**4.570919**	**3.601423**
5	1.77	7.92	3.9	1.08	**7.234504**	**6.148756**	**5.063007**
6	2.45	8.86	5.67	1.03	**8.791878**	**7.752699**	**6.713521**
7	3.18	8.13	5.09	0.79	**7.475465**	**6.683313**	**5.891161**
8	2.75	10.6	5.28	1.11	**8.603253**	**7.494508**	**6.385763**
9	1.68	10.35	4.97	1.24	**8.703288**	**7.459669**	**6.21605**
10	0.59	4.8	1.89	0.6	**3.733525**	**3.122346**	**2.511167**
11	1.26	4.08	2.49	0.46	**3.893431**	**3.428483**	**2.963536**
12	1.17	4.5	2.82	0.48	**4.261629**	**3.780601**	**3.299573**
13	1.06	4.5	1.98	0.47	**3.406009**	**2.931771**	**2.457533**

Table (6): Statistical analysis of equivalent Uranium distribution in (ppm) for each zone in East WadiLigan area.

Zones	Min.	Max.	Mean	S.D.	X+3 S.D.	X+2 S.D.	X+S.D.
1	7.36	31.06	20.00	4.06	32.1924	28.13028	24.06815
2	14.68	63.85	32.31	9.89	61.9876	52.09522	42.20283
3	5.38	37.17	18.50	4.12	30.86154	26.74269	22.62384
4	2.12	21.96	12.19	3.21	21.83145	18.62021	15.40897
5	3.44	22.77	11.63	3.26	21.39986	18.14306	14.88626
6	9.71	23.61	15.69	2.13	22.10512	19.96931	17.8335
7	9.63	27.48	17.86	3.25	27.60719	24.35812	21.10906
8	4.96	34.01	15.20	3.31	25.1237	21.81605	18.50839
9	10.17	76.83	33.77	13.36	73.85882	60.49615	47.13349
10	11.39	84.08	34.82	17.72	87.98207	70.26326	52.54444
11	8.14	36.96	20.74	4.11	33.08918	28.97458	24.85997
12	1.54	30.16	15.99	2.98	24.94424	21.9597	18.97516
13	6.73	21.77	14.13	2.35	21.18144	18.82997	16.47851

Table (7): Statistical analysis of equivalent Thorium distribution in (ppm) for each zone in East WadiLigan area.

Zones	Min.	Max.	Mean	S.D.	X+3 S.D.	X+2 S.D.	X+S.D.
1	32.89	86.19	58.89	10.80	91.30573	80.50289	69.70006
2	39.29	279.82	103.54	51.99	259.5372	207.539	155.5408
3	24.89	99.77	56.47	10.97	89.38206	78.41063	67.43919
4	18.47	49.16	31.34	5.94	49.15507	43.21624	37.27741
5	11.07	49.08	24.92	6.37	44.04297	37.66699	31.29101
6	12.80	45.22	26.64	5.00	41.6376	36.63737	31.63715
7	17.91	51.53	30.71	4.98	45.66507	40.68143	35.6978
8	12.68	54.25	25.76	6.29	44.63026	38.33886	32.04747
9	11.09	65.49	33.88	8.24	58.62013	50.37514	42.13014
10	1.85	35.26	12.52	4.66	26.5149	21.8519	17.1889
11	9.73	29.18	17.46	3.15	26.90731	23.75984	20.61237
12	6.70	32.08	18.29	3.22	27.95217	24.73106	21.50995
13	4.29	26.21	13.49	3.30	23.39282	20.09085	16.78887

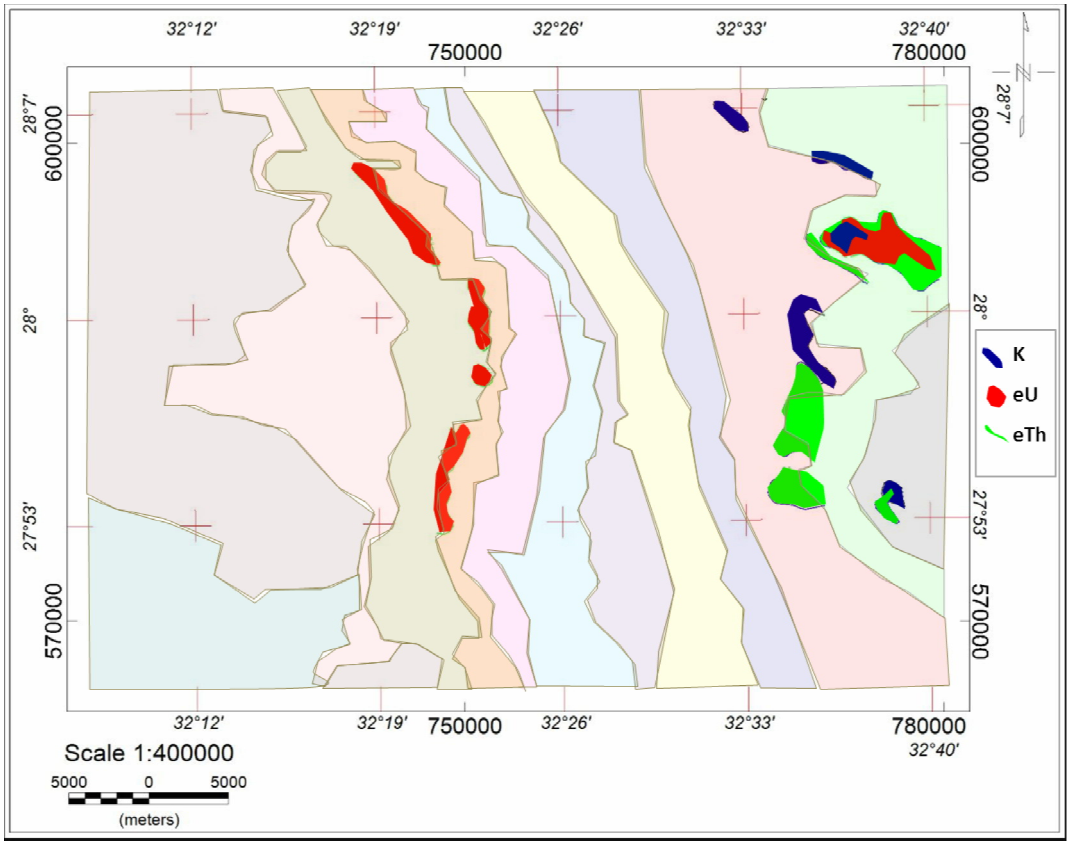

Fig. 11: Radioelement Leads Map, of the East WadiLigan Area, Central Eastern Desert, Egypt.

4.1.3. Identification of radioelements leads:

The major objective of the interpretation of the airborne gamma-ray spectrometric survey data is to define the probable locations and boundaries of potential nuclear provinces in which the rocks and soils are preferentially enriched in Potassium , Uranium and Thorium. This could be given by the following expression:

K > X+3S

eU > X+3S

eTh > X+3S

Where: "X" is the arithmetic mean and "S" is the standard deviation.

If the values of (X+3S) exceeded than the maximum value for each zone, it can't be used and then we use (X+2S), if it exceeded, we use (X+S). Here, (X+2S) is used in contouring for the three radioelements anomalies in some selected zones that represent the highest concentrations in each radioelement (Marked by red color in tables 5, 6 and 7).

Tables (5, 6 and 7) show the statistical results for the airborne spectrometric data of K , U and Th respectively.

Potassium leads: Donated as blue colour in the Radioelement Leads Map (Fig. 11). The most prevalent K leads located in the eastern side of the study area and are highly correlated with Wadi deposits which are represented by gravels of different sizes in sandy, limy and clayey matrix and some scatter parts in the basement rocks which are characterized by high radioactive content.

Uranium Leads: Uranium leads are coloured in the radioelement leads map as red color (Fig. 11). The majority of them are correlated with the Upper Cretaceous, Campanian (kur) Rakhiyat Formation, which are characterized by marginal marine shale and sandstone with marine carbonate and occasional phosphate beds. This formation is characterized by tidal and shallow marine deposits in the central part of the area, and also with the Upper Cretaceous, Maastrichtian (kus) Sudr Formation, which is characterized by uniform marine chalk with thin shale intercalations at the top ; locally flint concretions replaces Dakhla Formation. The remaining Uranium leads are correlated with the basement rocks which are characterized by high radioactive content and are located in the eastern side of the study area.

Thorium leads: Thorium leads are coloured by green color in the radioelement leads map (Fig. 11). It is associated with the basement rocks which are characterized by high radioactive content and Wadi deposits which are represented by gravels of different sizes in sandy, limy and clayey matrix and located in the eastern side of the study area. This Thorium-enriched

represents a good prospect for heavy mineral placer deposits and for rare earth deposits (Duval, 1983).

Most the radioelement anomalies have the NW-SE, N-S and NE-SW directions in the central parts of the study area. While the radioelement anomalies of the eastern part in the study area have the E-W, NW-SE and N-S directions. The radioelement anomalies are highly correlated with surface geologic map (Fig. 4).

5. CONCLUSIONS

From the analysis steps mentioned before we can conclude that:

1. The study area are covered nearly 70% by lower Cretaceous deposits in central and western parts while the basement complex rocks (granites, metavolcanics and dokhanvolcanics) lie in the eastern side and the other parts are filled with Quaternary deposits.
2. Airborne radiometric data are subjected to some processing to get the radioelement composite image (Fig. 9) Combines the data for eU (in red), eTh (in green), and K (in blue) and then divided it based on colour difference into thirteen visible zones which show to great extend similarity between the gamma-ray spectrometry data and the geology .
3. Applying some statistical tests on the derived zones starting by the coefficient of variation which proves that every zone separately represents a homogeneous unit.
4. Applying the bartlett's test on 11 groups proves that these units were considered to possess heterogeneous variances in terms of radioactivity and can't be grouped together.
5. Applying the Fisher's test on the 12 couples on TC radiometric data proves that 11 couples were accepted. The remaining couple was considered to possess heterogeneous variances in terms of radioactivity.
6. Applying the Student's test on the 11 couples on TC radiometric data that are accepted in the Fisher's test proves that all the 11 couples were rejected and any zones can't be gathered together.
7. Constructing a radioelement leads map represents the concentration of each radioelement (K , eU & eTh) and compare it with the surface geology map which are highly correlated with the radioelement anomalies.

REFERENCES

Aero-Service (1984)*:* Final operational report of airborne magnetic/radiometric survey in the Eastern Desert, Egypt. For the Egyptian General Petroleum Corporation: Aero-Service, Houston, Texas, USA, six volumes.

Conoco Coral and EGPC (1987): Geological map of Egypt, scale 1:500,000.

Dixon, W.J. and Massey, F.J. (1957): Introduction to statistical analysis Secondedition, McGraw-hill book company, Inc.,Newyork,Toronto,London, 488 P.

Duval, J.S. (1983): Composite color images of aerial gamma-ray spectrometric data. Geophysics, 48/6, 722-735.

El-Tarabili, S. (1964): General outlines of the structures of the sedimentary formations in the Central part of the Eastern Desert of Egypt, Safaga-Quseir- WadiQena southern part. Bull. Inst. Desert Egypt, V. 14, pp. 27-39.

Everitt, Brian (1998): The Cambridge Dictionary of Statistics. Cambridge, UK New York: Cambridge University Press. ISBN 0521593468.

Geigy, I.R. (1962): DocumentaGeigy scientific tables. 6th ed., edited by Konrad Diem, published by Geigy, I. R., Basle, S. A., Switzerland.

Grasty, R.L., and Darnly, A.G. (1970): The calibration of gamma-ray spectrometers for ground and aiborne use. Geol. Surv. of Canada, paper 17-77, 27 p.

International Atomic Energy Agency (1991): Airborne gamma-ray spectrometer survey. Technical reports series No. 323, IAEA, Vienna, 97 p.

Meshref, W.M. (1990): Tectonic framework, the geology of Egypt (Chapter VII), Ed. R. Said, Balkema, Rotterdam, Book field, 1990.